Effect of Nb on microstructure and mechanical properties of 700 MPa grade truck beam steel

M. Y. Sun, X. L. Wang, X. M. Wang*

Collaborative Innovation Center of Steel Technology, University of Science and Technology Beijing, Beijing 100083, P. R. China

Abstract

700 MPa grade Ti and Nb-Ti microalloyed steels were developed to study the effect of Nb on the microstructure and mechanical properties in truck beam steels. The microstructure in Ti microalloyed steel mainly consisted of ferrite, bainite, and pearlite. In contrast, the microstructure of Nb-Ti microalloyed steel was characterized by bainite and low volume fraction of ferrite. Moreover, there was a large volume fraction of nano precipitates and coarse TiN inclusions in both the steels because of high Ti content. The TiN inclusion, together with coarse-grained ferrite, is detrimental to the toughness of steels. This influence is weakened by the addition of Nb because of the remarkable effect on grain refinement. The effective grain size in Ti and Nb-Ti steels was 4.2 and 2.2 µm, respectively. As a consequence, although the strength of the two steels was similar, the impact toughness of Nb-Ti steel was significantly better than that of Ti steel. Additionally, the uniformity in tensile properties of Nb-Ti steel was higher than that of Ti steel, which is beneficial for improving product pass rate and processing.

K e y   w o r d s: Nb, truck beam steel, microstructure, precipitation, mechanical properties

1. Introduction

High strength truck beam steel has received extensive attention due to the rapid development of the heavy-duty truck industry [1]. Instead of heavy plates, the use of high strength thin plates can reduce the amount of steel used and improve transport efficiency at the same time [2–4]. The truck beam steel is widely used as a load-bearing plate. However, there are only a few studies on the truck beam steels with high yield strength [5, 6].

Truck beam steels are required to offer a remarkable combination of high strength and toughness to meet safety standards. Titanium can refine austenite grain and improve the strength along with precipitation strengthening. Besides, Ti-Fe is cheaper than other alloying elements. Therefore, Ti microalloyed high strength steels have been developed to lower the cost [7–10]. The addition of Ti in steel can result in fine TiN and TiC precipitates, which can inhibit austenite grain growth at high temperature and

increase strength, respectively. However, the coarse TiN inclusions formed during solidification, together with coarse-grained ferrite, may cause cleavage fracture [11].

It is well known that grain refinement is a practical approach to improve strength and toughness simultaneously [12]. Thermo-mechanical controlled process (TMCP) was usually used for grain refinement, and niobium has an essential role during hot rolling. Nb is one of the most effective microalloying elements that retards austenite recrystallization during TMCP [13, 14]. The microstructure can be refined after phase transformation due to strain accumulation during hot rolling caused by the retardation of recrystallization [15]. Thus, we envisage that the toughness of Ti microalloyed steel can be enhanced by the addition of Nb. To lower cost, high strength microalloyed steel with low carbon and niobium, high titanium is designed, and other alloying elements are reduced. Therefore, our objective here is to elucidate the effect of Nb on microstructure and mechanical prop-

*Corresponding author: e-mail address: wxm@mater.ustb.edu.cn

T a b l e 1. Chemical composition of the material (wt.%)

Steels	C	Si	Mn	Nb	Ti	N	P	S
Nb-Ti	0.07	0.10	1.5	0.03	0.08	0.0034	0.012	0.002
Ti	0.08	0.10	1.6	–	0.11	0.0035	0.010	0.002
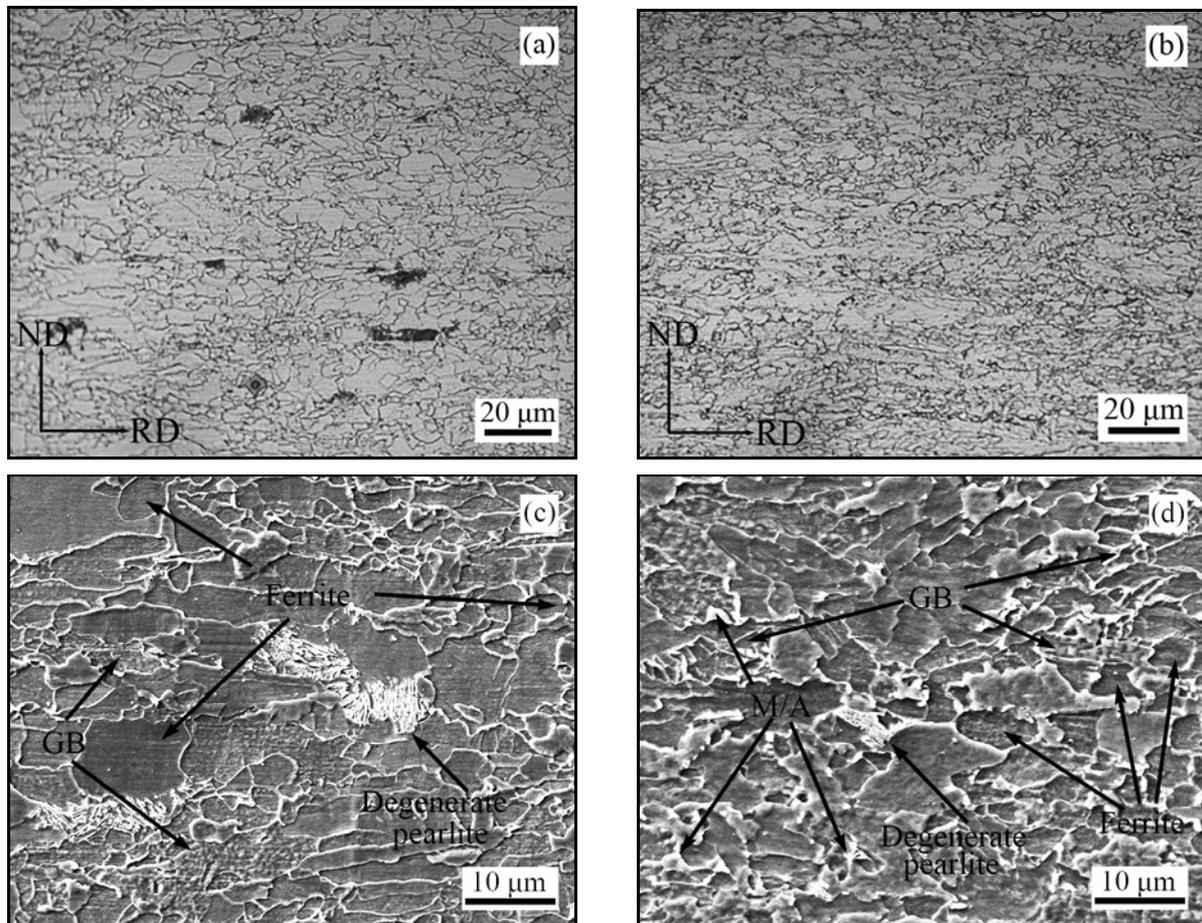
Fig. 1. Optical and SEM micrographs of experimental steels: (a), (c) Ti steel; (b), (d) Nb-Ti steel.

erties in 700 MPa Ti microalloyed truck beam steel.

2. Experimental

The present work was carried out on 700 MPa Ti and Nb-Ti truck beam steels with a thickness of 10 mm. The steels were rolled via a series of passes at 1050–960 °C and 890–850 °C, and the plates were coiled at 600 °C. Table 1 shows the chemical composition of the experimental steels. Higher Ti content is designed in Ti microalloyed steel without Nb to meet the strength requirement by precipitation strengthening.

Tensile and Charpy V-notch (CVN) impact specimens were cut from the as-rolled plates in the rolling direction. Tensile tests were conducted at a constant crosshead speed of 3 mm/min. Three tensile specimens were tested for each steel. CVN specimens with dimensions of 55 mm × 10 mm × 7.5 mm were tested at –20 °C.

For optical microscopy (OM) and scanning electron microscopy (SEM), the samples were etched with 4 % nital after mechanical polishing. Transmission electron microscopy (TEM) foils were twin-jet electropolished to perforation using a solution of 5 % perchloric acid and 95 % ethanol at –20 °C after mechanically thinning to 50 μm. JEOL JEM-2100 TEM operated at 200 keV was used for examining the foils. Samples for electron back-scattering diffraction (EBSD) were prepared by electrolytic polishing using a solution containing 10 % perchloric acid, 5 % glycerol, and 85 % alcohol. EBSD data was obtained by orientation imaging microscopy (OIM) under the following conditions:

acceleration voltage, 20 kV; working distance, 15 mm; tilt angle, 70°; step size, 0.05 μm. Channel 5 software from Oxford-HKL was employed for post-processing orientation data. The number and composition of inclusions in samples were quantitatively analyzed by automatic inclusion analysis (EVO18-INCA steel).

3. Results and discussion

3.1. Microstructure

Optical and SEM micrographs of the experimental steels are shown in Fig. 1. It can be seen from Figs. 1a,b that in both steels the microstructure mainly consisted of ferrite and bainite. Also, degenerate pearlite was observed in Ti steel. The SEM micrographs show that the microstructure of Ti steel consisted of ferrite, a small amount of bainite, and degenerate pearlite (Fig. 1c). It has been reported that it is detrimental to the toughness of steel when there is more than a 5 % volume fraction of the brittle phase in steel, such as cementite, pearlite, martensite, etc. [16, 17]. Thus, the brittle degenerate pearlite in Ti steel may have a negative effect on toughness. The microstructure of Nb-Ti steel is characterized by bainite together with some fine martensite/austenite (M/A) constituents (Fig. 1d) and a small amount of ferrite (Fig. 1d). Although there is also degenerate pearlite in Nb-Ti steel indicated by an arrow in Fig. 1d, it has little effect on toughness due to its small volume fraction and size. Moreover, it can be seen from Fig. 1c that the microstructure in Ti steel is inhomogeneous, and a few ferrite grains are even larger than 10 μm. However, it was reported that grain size heterogeneity had a negative effect on toughness [18]. In contrast, the microstructure of Nb-Ti steel is homogeneous and characterized by finer ferrite and more bainite, attributing to the effect of Nb on delaying ferrite transformation. The results show that the addition of Nb in truck beam steel can decrease the volume fraction of ferrite and pearlite and refine ferrite grain size effectively.

Figure 2 illustrates boundary distribution and effective grain size distribution measured by EBSD for experimental steels. Figures 2a,b show that the density of high angle boundaries ($\theta > 15°$) in Nb-Ti steel is higher than in Ti steel. It was reported that high angle grain boundaries could effectively impede crack propagation, which is beneficial to improve the toughness of steels [19, 20]. The effective grain size (enclosed by boundaries with misorientation larger than 15°) was analyzed by EBSD, as shown in Fig. 2c. The results show that the frequency of grains with small size in Nb-Ti steel is higher than in Ti steel. The average size of effective grains in Nb-Ti steel (2.2 μm) is significantly smaller compared with Ti steel (4.2 μm),
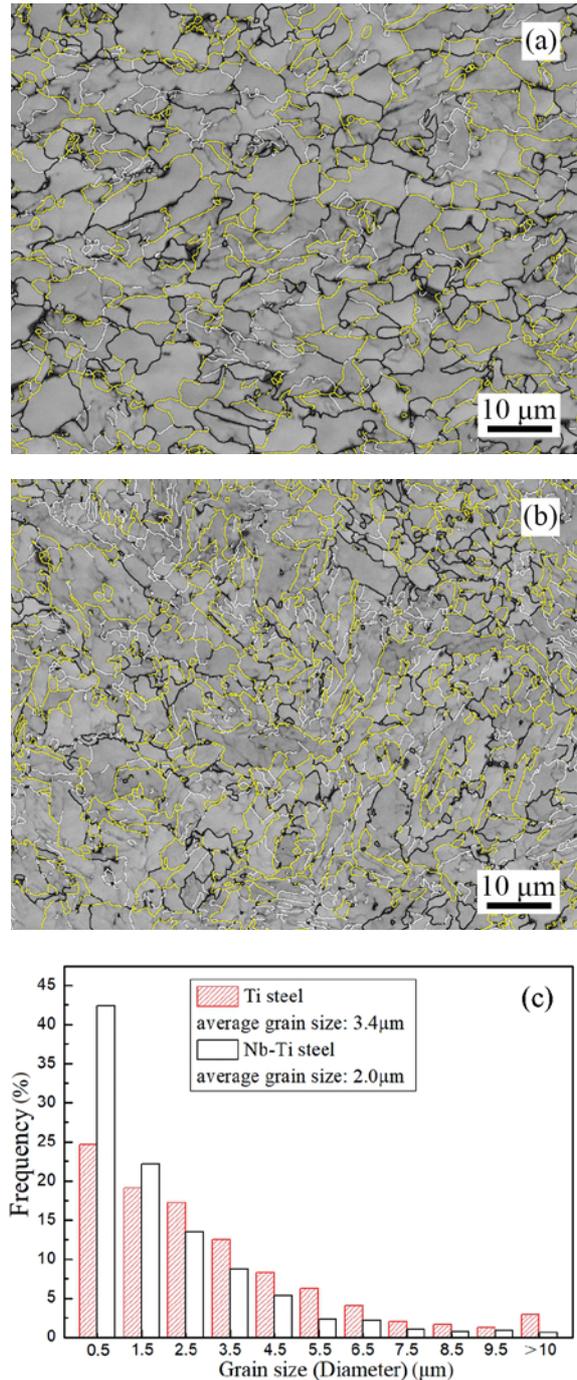
Fig. 2. Boundary distribution and effective grain size distribution measured by EBSD in experimental steels: (a), (b) boundary distribution in Ti steel and Nb-Ti steel, respectively (white line: $5° < \theta < 15°$, black line: $15° < \theta < 45°$, yellow line: $\theta > 45°$; θ – misorientation); (c) effective grain size ($\theta > 15°$) distribution in experimental steels.

which can impede crack propagation more effectively and improve toughness.

Figure 3 shows the TEM micrographs of the studied samples. Typical ferrite with a low density of dis-
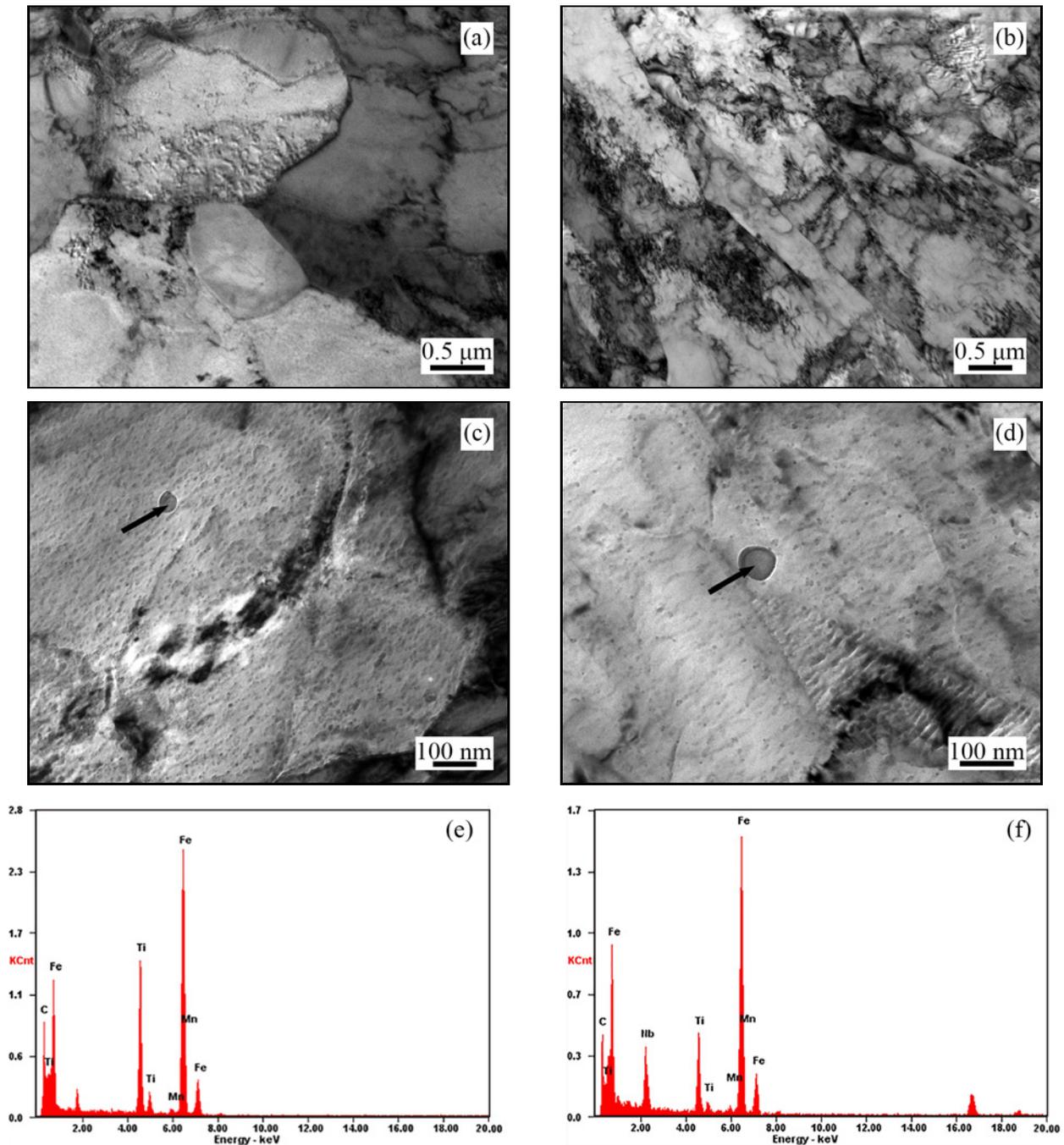
Fig. 3. TEM micrographs of experimental steels. (a), (b) microstructure of Ti steel and Nb-Ti steel, respectively; (c) TiC precipitate indicated by a black arrow in Ti steel; (d) (Ti,Nb)C precipitate indicated by a black arrow in Nb-Ti steel; (e), (f) corresponding EDS analysis of precipitates in Ti and Nb-Ti steels, respectively.

location can be observed in Ti steel (Fig. 3a), while bainite lath was observed in Nb-Ti steel (Fig. 3b). Some precipitates of size ~ 50–200 nm were found in Figs. 3c,d, and the corresponding Energy Dispersive Spectrometer (EDS) analysis indicates that these precipitates are TiC (Fig. 3e) in Ti steel and (Ti,Nb)C (Fig. 3f) in Nb-Ti steel.

A large amount of fine precipitates was obtained in ferrite, as shown in Fig. 4. These precipitates were

considered to be TiC or (Ti,Nb)C due to their size, the thermomechanical processing, and composition of the experimental steels. It can be seen from Figs. 4a,b that the amount of fine precipitates, especially interphase precipitates in Ti steel, is more extensive than in Nb-Ti steel. This is attributed to the higher Ti content in Ti steel. The interphase precipitation occurs during γ/α-phase transformation, and more ferrite grains nucleated and grew during the coiling process in Ti
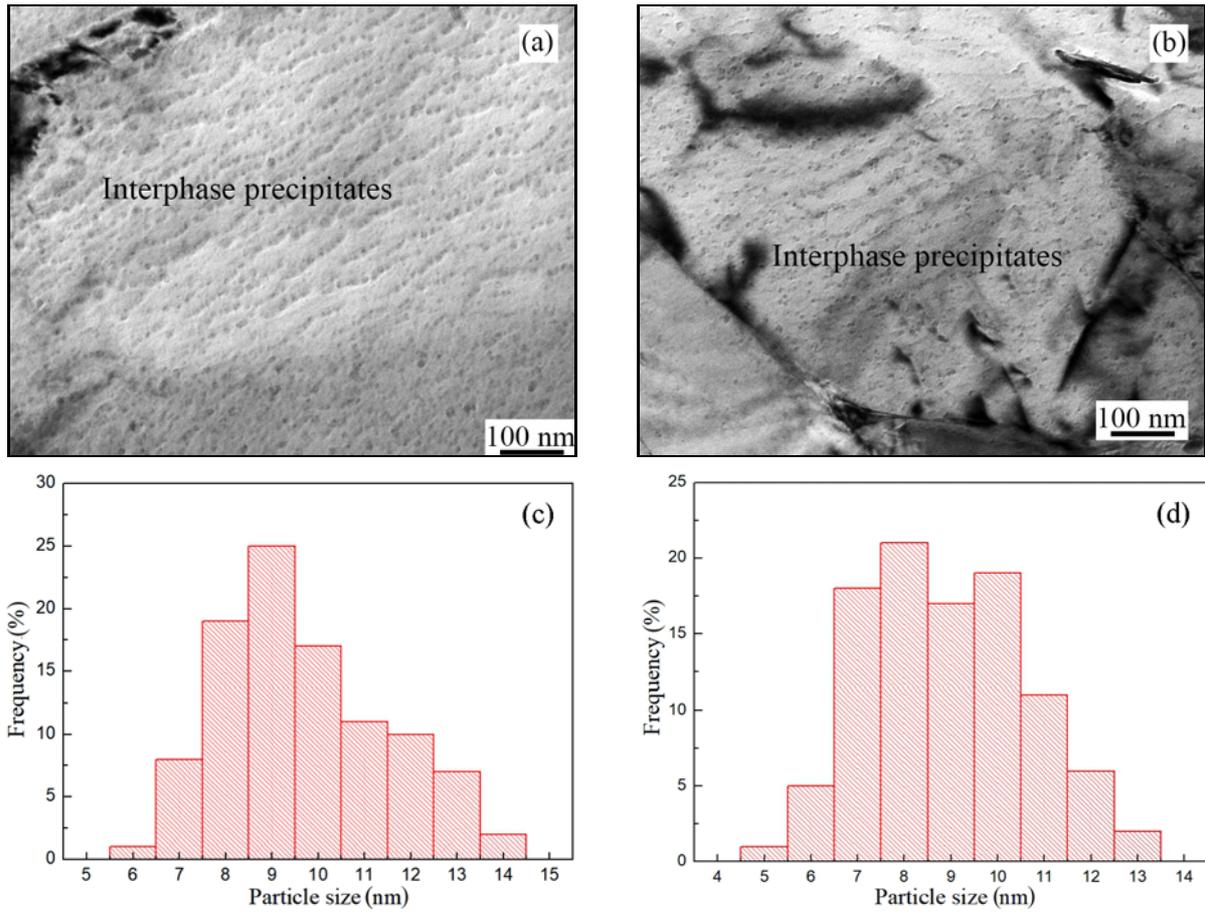
Fig. 4. Fine precipitate morphology and diameter distribution of experimental steels. (a), (b) fine precipitates in Ti and Nb-Ti steels, respectively; (c), (d) diameter distribution of fine precipitates in Ti and Nb-Ti steels, respectively.

steel also promoted the formation of interphase precipitates.

The diameter distribution of fine precipitates is summarized in Figs. 4c,d. Although the size of precipitates ranged from 3 to 12 nm in diameter, the average size of these fine precipitates in Nb-Ti steel (5.8 nm) is slightly finer than in Ti steel (6.1 nm). Meanwhile, the volume fractions of fine precipitates were measured, and they were 0.0044 and 0.0021 in Ti and Nb-Ti steels, respectively.

3.2. Inclusion analysis

Non-metallic inclusions can cause crack initiation and propagation, which is detrimental to mechanical properties [21]. It is important to analyze the inclusions in steels; thus, the number and composition of inclusions with the size larger than 1 μm have been quantitatively analyzed by automatic inclusion analysis (EVO18-INCA steel).

The primary inclusions in the experimental steels are TiN, oxide, sulfide, or oxide-sulfide composite inclusions, and the frequency of these inclusions is presented in Fig. 5. The result shows that TiN accounted
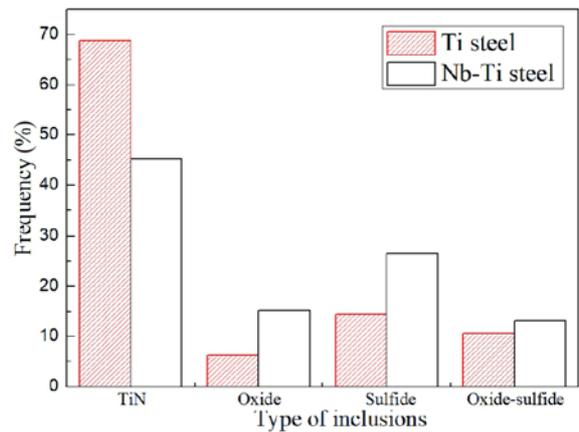
Fig. 5. Frequency of different types of inclusions in experimental steels.

for the most substantial proportion, and the frequency of TiN inclusions in Ti steel is 69 %, while the frequency of TiN inclusions in Nb-Ti steel is 45 %.

Figure 6 shows the element maps of typical TiN inclusions in Ti steel. In Fig. 6a, there are no other el-
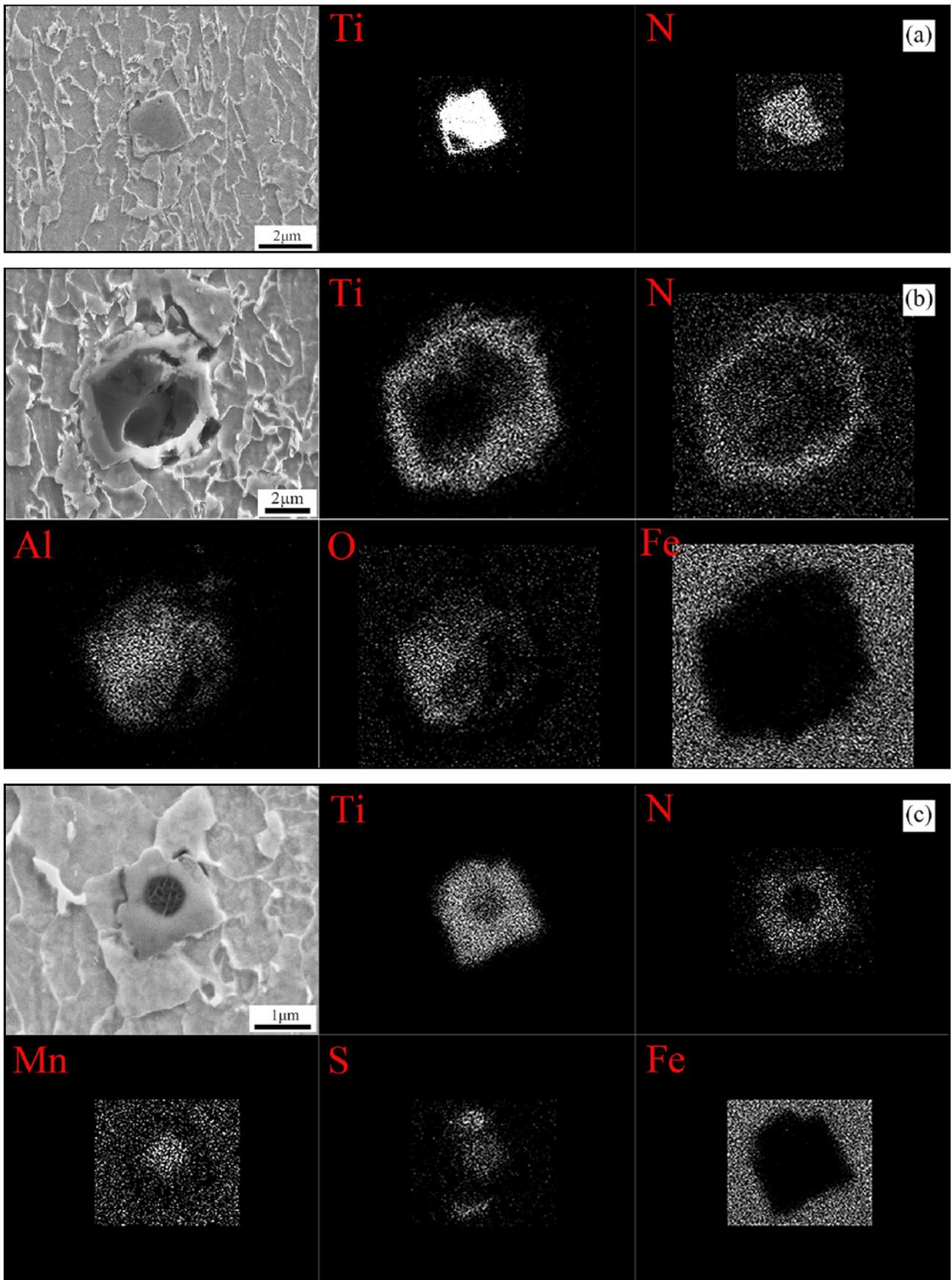
Fig. 6. SEM element mappings of typical coarse TiN particles in Ti steel: (a) TiN particle without other inclusions inside, (b) TiN particle nucleated on Al_2O_3 inclusion, and (c) TiN particle nucleated on MnS inclusion.
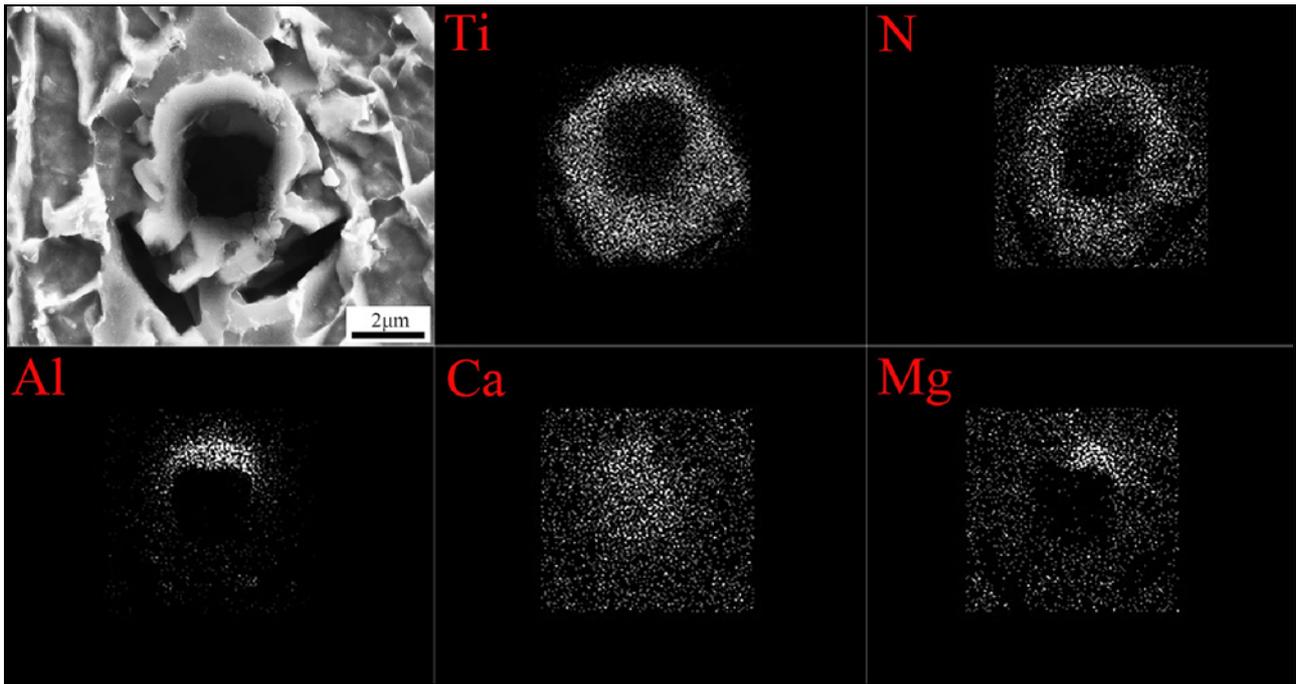
Fig. 7. SEM element mappings of coarse TiN particles nucleated on Al-Ca-Mg complex inclusion in Nb-Ti steel.

T a b l e 2. Number and density of inclusions in experimental steels

Steels	Total number	Scanned area (mm^2)	Density (mm^{-2})
Nb-Ti	1128	39.6	28.6
Ti	1364	39.6	34.4

T a b l e 3. Mechanical properties of experimental steels

Steels	R_{eL} (MPa)	R_{m} (MPa)	A_{25} (%)	A_{kv} (–20 ℃) (J)
Ti	722	783	21.6	11/21/43
Nb-Ti	705	780	24.8	117/88/89

ements inside the TiN inclusion with a square shape. TiN inclusions often formed on oxide, sulfide inclusions. The Al$_2$O$_3$-TiN complex inclusion is characterized by the coarse TiN inclusion formed on the Al$_2$O$_3$ inclusion, as shown in Fig. 6b. In Fig. 6c, the MnS-TiN inclusion consists of MnS in the inner part and TiN in the outer layer. TiN inclusions are also present in Nb-Ti steel and TiN inclusion formed on irregular Al-Ca-Mg complex inclusion, as shown in Fig. 7. It can be seen from the element maps that the TiN inclusions often formed on other inclusions. The higher Ti content in Ti steel can increase the amount of these TiN complex inclusions; as a result, the frequency of TiN inclusions in Ti steel is higher than in Nb-Ti steel.

The total number and density of inclusions obtained from the same selected area are illustrated in Table 2, indicating that the density defined as the number per unit area in Ti steel is higher than in Nb-Ti steel. It means that more inclusions existed in Ti steel, especially TiN inclusions. A large amount of coarse TiN inclusions in experimental steels can reduce toughness and ductility.

3.3. Mechanical properties

Table 3 shows the mechanical properties of the experimental steels. Compared with Nb-Ti steel, the yield strength of Ti steel is slightly higher, while the Charpy impact energy at –20 ℃ is lower. Although there is more ferrite in Ti steel than in Nb-Ti steel, the higher yield strength of Ti steel is because of significant precipitation strengthening.

The contribution of precipitation hardening to
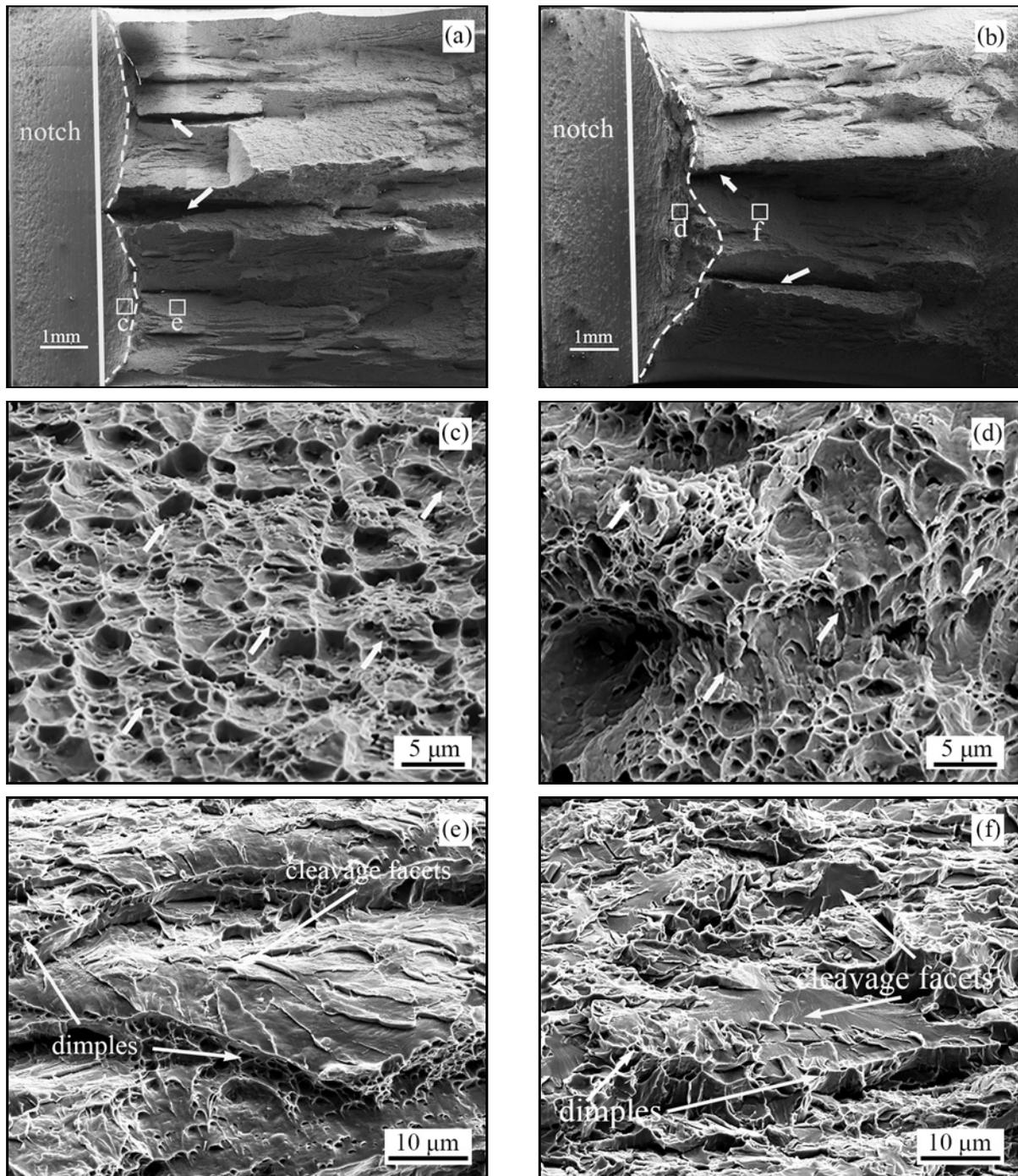
Fig. 8. (a), (b) SEM micrographs of the fracture surface of Ti and Nb-Ti steels, respectively, ductile zones of dimples are circled by white dashed lines; (c), (e) the magnified SEM micrographs of the selected areas marked by 'c', and 'e' in (a), respectively; (d), (f) the magnified SEM micrographs of the selected areas marked by 'd', and 'f' in (b), respectively.

yield strength is calculated by Ashby–Orowan [22]:

$$\sigma_{\mathrm{p}} = \frac{5.9\sqrt{f}\ln(X/0.00025)}{X}, \qquad (1)$$

where f and X are the volume fraction and diameter (μm) of the precipitates, respectively. According to the volume fraction and size of precipitates, the

yield strength of Ti and Nb-Ti steels was calculated to be 205 and 146 MPa, respectively. The precipitation strengthening in Ti steel is stronger than in Nb-Ti steel because of higher Ti content in Ti steel.

The Charpy impact energy of Ti steel is much lower than of Nb-Ti steel, which is related to the microstructure. The inhomogeneous ferrite grains and brittle degenerate pearlite in Ti steel are detrimental to impact

toughness. In contrast, Nb-Ti steel has a homogeneous and finer ferrite, and the effective grain size is smaller than in Ti steel.

3.4. Impact fracture morphology

Figure 8 shows the fracture surface of the experimental steels. The Ti sample with Charpy impact energy of 43 J and Nb-Ti sample with Charpy impact energy of 89 J were selected to examine the morphology of the fracture by SEM. It can be seen from Figs. 8a,b that the ductile zone of dimples along the notch root in Nb-Ti sample is much wider than in Ti sample. The ductile zone is wider, the plastic deformation before cleavage crack initiation in the material is larger, which is the main reason for better toughness in Nb-Ti steel. It can be seen from Figs. 8c,d that there are many small dimples in the ductile fracture zone of the studied samples, and some of them contain fine particles indicated by white arrows, which means that micro-voids can nucleate around particles.

Because of the high density of precipitates in studied samples, a large number of micro-voids nucleated around the particles, which limited the growth of dimples, thus the ductile zone consisted of many small and shallow dimples, as shown in Figs. 8c,d. It can be seen that both the samples exhibit quasi-cleavage fracture and small dimples in shear ridges can be observed, as shown in Figs. 8e,f. Moreover, the cleavage facet size of Nb-Ti sample is significantly smaller than of Ti sample, which is related to the smaller effective grain size in Nb-Ti steel. Luo's study indicated that the local cleavage fracture stress increased with decreasing cleavage facet size [23]. It is known that cleavage fracture may occur when the stress at the front of the crack tip exceeds the cleavage fracture stress. Therefore, when the cleavage fracture stress is high, the plastic deformation before cleavage crack initiation in a material is large due to the difficulty in the initiation of cleavage fracture. According to the above analysis, the Charpy impact energy of Nb-Ti steel is higher than Ti steel due to its smaller effective grain size.

3.5. Stability of mechanical properties

The use of steel plates with high strength is the most important way of reducing weight and improving the safety of the truck beam. However, the variation in mechanical properties of high strength steel plates causes changes in processing performance, and it is difficulty of the fabrication of truck beam and control accuracy.

Industrial production of 700 MPa Ti and Nb-Ti microalloyed steel plates were completed, and 100 plates of each steel were selected to study the mechanical properties uniformity. Figure 9 shows the strength and

elongation distribution of Ti and Nb-Ti steels. It can be seen from Fig. 9a that the yield strength of Ti steel is 620–840 MPa, its variation is ∼ 220 MPa, and the average yield strength is ∼ 720 MPa. The yield strength of Nb-Ti steel is 640–770 MPa, and the average yield strength is ∼ 710 MPa, as shown in Fig. 9b. In contrast, the yield strength variation of Nb-Ti steel is only ∼ 130 MPa, which is about 60 % the value of Ti steel.

For Ti and Nb-Ti steels, both the tensile strength and yield strength distribution show a similar tendency. It can be seen from Fig. 9c that the tensile strength of Ti steel is 680–920 MPa, its variation is ∼ 240 MPa, and the average tensile strength is ∼ 780 MPa. The tensile strength of Nb-Ti steel is 710–830 MPa, and the average tensile strength is ∼ 770 MPa, as shown in Fig. 9d. The tensile strength variation of Nb-Ti steel is only ∼ 120 MPa, which is 50 % the value of Ti steel.

Figures 9e,f show variation in elongation of Ti and Nb-Ti steels. The elongation of Ti steel is 15–28 %, and the average elongation is ∼ 20.5 %, while the elongation of Nb-Ti steel is 16–30 % and the average elongation is ∼ 21.9 %. It is clear that the elongation of Nb-Ti steel is higher than that of Ti steel. The elongation of Nb-Ti steel is higher than that of Ti steel, which is easy to form.

The uniformity of the tensile performance of Nb-Ti steel is higher than that of Ti steel, which is beneficial for improving the formability of steels. It is known that the coiling temperature and cooling rate vary in different coils or different positions of the same coil, which will significantly affect the TiC precipitation behavior and, consequently, mechanical properties uniformity. According to the result of the calculation of the precipitation strengthening, we know that the precipitation strengthening is stronger in Ti steel than in Nb-Ti steel, which may result in a higher variation of yield strength in Ti steel.

4. Conclusions

1. The microstructure of Ti microalloyed steel consists of ferrite with inhomogeneous grain size, a small amount of bainite and degenerate pearlite, together with a high volume fraction of fine precipitates. In contrast, the microstructure of Nb-Ti microalloyed steel is characterized by bainite and low volume fraction of ferrite. The effective grain size is 4.2 μm in Ti steel and 2.2 μm in Nb-Ti steel. The addition of Nb in Ti steel can decrease the amount of ferrite and pearlite, and refine effective grain size effectively. Additionally, the number of coarse TiN inclusions in Ti steel is more than in Nb-Ti steel.

2. The yield strength of Ti steel is similar to that of Nb-Ti steel, while the Charpy impact energy of Nb-Ti
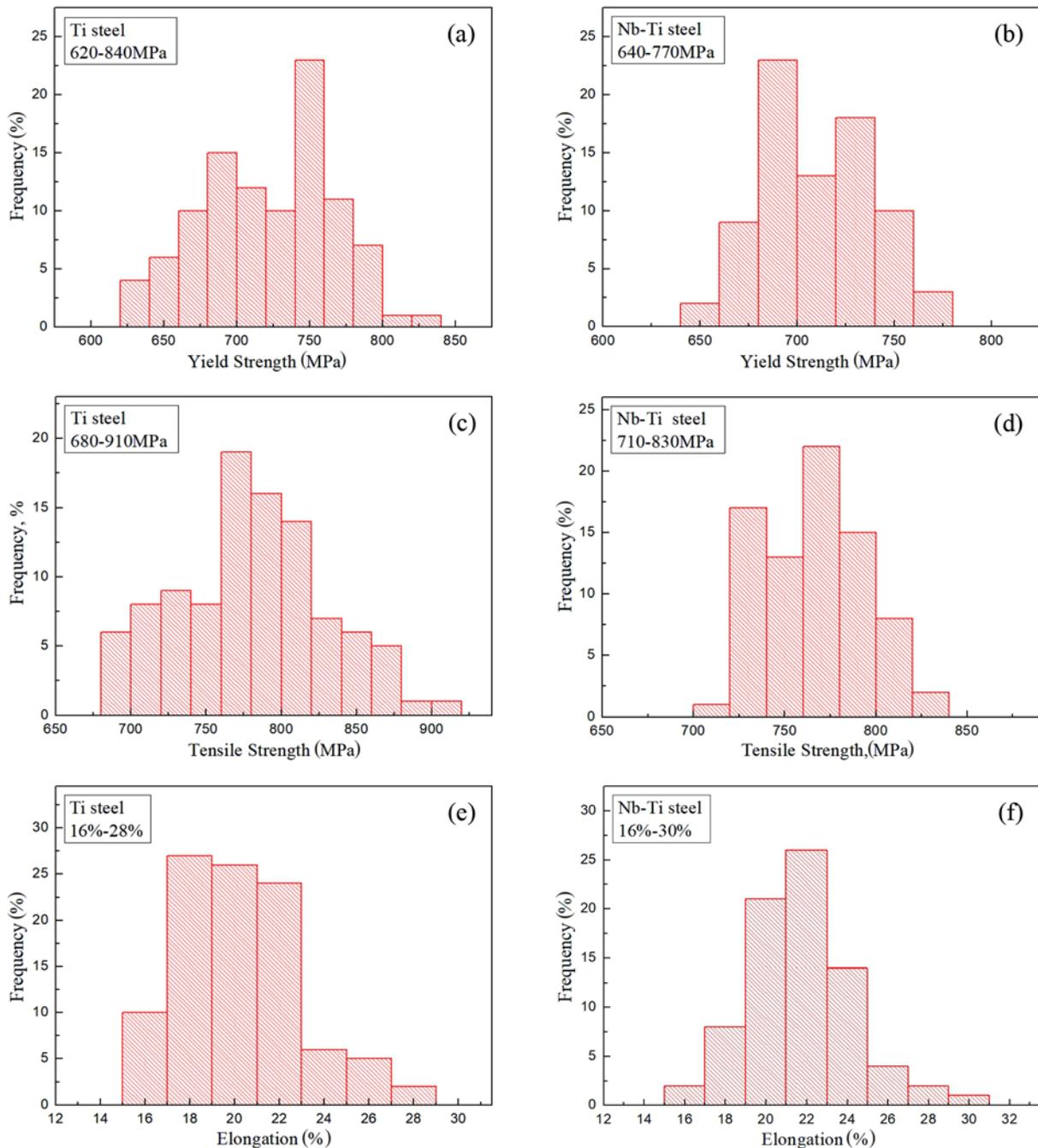
Fig. 9. (a), (b) Yield strength distribution of Ti and Nb-Ti steels, respectively; (c), (d) tensile strength distribution of Ti and Nb-Ti steels, respectively; (e), (f) elongation distribution of Ti and Nb-Ti steels, respectively.

steel is significantly higher. The number of fine precipitates, especially interphase precipitates in Ti steel, are higher than in Nb-Ti steel, and the contribution of precipitation strengthening to yield strength was estimated to be 205 MPa and 146 MPa in Ti and Nb-Ti steels, respectively. Besides, the Charpy impact energy of Nb-Ti steel is higher than that of Ti steel because of its smaller effective grain size.

3. The uniformity of mechanical properties and elongation of Nb-Ti steel are higher than those of Ti

steel, which is beneficial for improving the formability of steels.

References

[1] A. Klimová, J. Lapin, Effect of Al content on microstructure of Ti-Al-Nb-C-Mo composites reinforced with carbide particles, Kovove Mater. 57 (2019) 377–387. doi:10.4149/km_2019_6_377

[2] W. Strunk Jr., E. B. White, The Elements of Style, 4th ed., Longman, New York, 2000.

[3] H. A. Dabkowska, A. B. Dabkowski, R. Hermann, J. Priede, G. Gerbeth, Floating Zone Growth of Oxides and Metallic Alloys Handbook of Crystal Growth. In: P. Rudolph (Ed.), Handbook of Crystal Growth, Elsevier, Oxford, 2015, pp. 281–329.

[4] J. Ekengard, A. Dioszegi, P. G. Jönsson, A study of the oxygen activity before start of solidification of cast irons, Proceedings of 10th International Symposium on the Science and Processing of Cast Iron, SPCI10 (2014), pp. 156–163. ISBN 978-987-45833-0-7.

[5] X. N. Wang, L. X. Du, H. L. Zhang, H. S. Di, Industrial trial of 780 MPa grade heavy-duty truck beams steels, J. of Iron and Steel Res. 23 (2011) 45–49.

[6] X. S. Li, Y. Yang, Y. X. Yang, H. Wu, Composition design of bainitic steel for heavy truck front axle beam with inequable cross-sections, Mater. Res. Innov. 17 (2013) 119–222. doi:10.1179/1432891713Z.000000000200

[7] F. Z. Bu, X. M. Wang, L. Chen, S. W. Yang, C. J. Shang, R. D. K. Misra, Influence of cooling rate on the precipitation behavior in Ti-Nb-Mo microalloyed steels during continuous cooling and relationship to strength, Mater. Char. 102 (2015) 146–155. doi:10.1016/j.matchar.2015.03.005

[8] H. L. Yi, L. Z. Long, Z. Y. Liu, G. D. Wang, Investigation of precipitate in polygonal ferrite in Ti-microalloyed steel using TEM and APT, Steel Res. Int. 85 (2014) 1446–1452. doi:10.1002/srin.201300230

[9] X. L. Li, F. Li, Y. Cui, B. L. Xiao, X. M. Wang, The effect of manganese content on mechanical properties of high titanium microalloyed steels, Mat. Sci. Eng. A 677 (2016) 340–348. doi:10.1016/j.msea.2016.09.070

[10] X. N. Wang, Y. F. Zhao, B. J. Liang, L. X. Du, H. S. Di, Study on isothermal precipitation behavior of nano-scale (Nb,Ti)C in ferrite/bainite in 780 MPa grade ultra-high strength steel, Steel Res. Int. 84 (2013) 402–409. doi:10.1002/srin.201200195

[11] W. Yan, Y. Y. Shan, K. Yang, Effect of TiN inclusions on the impact toughness of low-carbon microalloyed steels, Metall. and Mat. Trans. A 37 (2006) 2147–2158. doi:10.1007/BF02586135

[12] H. Beladi, I. B. Timokhina, X. Y. Xiong, P. D. Hodgson, A novel thermomechanical approach to produce a fine ferrite and low-temperature bainitic composite microstructure, Acta Mater. 61 (2013) 7240–7250. doi:10.1016/j.actamat.2013.08.029

[13] Vervynckt, S., Verbeken, K., Thibaux, P., Houbaert, Y.: Recrystallization-precipitation interaction during austenite hot deformation of a Nb microalloyed steel, Mat. Sci. Eng. A 528 (2011) 5519–5528. doi:10.1016/j.msea.2011.03.087

[14] C. Fossaert, G. I. Rees, T. Maurickx, H. K. D. H. Bhadeshia, The effect of niobium on the hardenability of microalloyed austenite, Met. Mat. Trans. A 26 (1995) 21–30. doi:10.1007/BF02669791

[15] J. Calvo, I. H. Jung, A. M. Elwazri, D. Bai, S. Yue, Influence of the chemical composition on transformation behaviour of low carbon microalloyed steels, Mat. Sci. Eng. A 520 (2009) 90–96. doi:10.1016/j.msea.2009.05.027

[16] S. Y. Han, S. Y. Shin, S. H. Lee, N. J. Kim, J. H. Bae, K. S. Kim: Effects of cooling conditions on tensile and Charpy impact properties of API X80 linepipe steels, Met. Mat. Trans. A 41 (2010) article no. 329. doi:10.1007/s11661-009-0135-4

[17] H. K. Sung, S. Y. Shin, B. Hwang, C. G. Lee, N. J. Kim, S. H. Lee, Effects of carbon equivalent and cooling rate on tensile and Charpy impact properties of high-strength bainitic steels, Mat. Sci. Eng. A 530 (2011) 530–538. doi:10.1016/j.msea.2011.10.015

[18] N. Kang, Y. Lee, S. Byun, K. Kim, J. Chung, K. Cho, Quantitative analysis of microstructural and mechanical behavior for Fe-0.1C-(V, Nb) steels as a function of the final rolling temperature, Mat. Sci. Eng. A 499 (2009) 157–161. doi:10.1016/j.msea.2007.11.145

[19] H. Kitahara, R. Ueji, N. Tsuji, Y. Minamino, Crystallographic features of lath martensite in low-carbon steel, Acta Mater. 54 (2006) 1279–1288. doi:10.1016/j.actamat.2005.11.001

[20] A. Lambert-Perlade, A. F.Gourgues, A. Pineau, Austenite to bainite phase transformation in the heat-affected zone of a high strength low alloy steel, Acta Mater. 52 (2004) 2337–2348. doi:10.1016/j.actamat.2004.01.025

[21] H. Tervo, A. Kaijalainen, T. Pikkarainen, S. Mehtonen, D. Porter, Effect of impurity level and inclusions on the ductility and toughness of an ultra-high-strength steel, Mat. Sci. Eng. A 697 (2017) 184–193. doi:10.1016/j.msea.2017.05.013

[22] T. Gladman, D. Dulieu, I. D. Mcivor, Structure-Property Relationships in High Strength Microalloyed Steels, Proceeding of Symposium on Microalloying, New York, 1976, pp. 32–34.

[23] M. Luo, D. S. Liu, B. G. Cheng, R. Cao, J. H. Chen, Mechanism of decrease in impact toughness in a low-carbon MnCrMoNiCu plate steel with increasing austenitizing temperature, J. Mat. Eng. Perform. 27 (2018) 4855–4870. doi:10.1007/s11665-018-3591-4